Articles

The Competition between Allene and Butadiene in the Carbon−Hydrogen Bond Activation Initiated by a Tungsten Allyl Complex: A DFT Study

Yubo Fan and Michael B. Hall*

Department of Chemistry, Texas A&M University, College Station, Texas 77843-3255

Received December 3, 2004

Mechanisms for H-transfer from 1,1-dimethylallyl (DMA) to neopentyl (CH_2t-Bu) in the complex Cp*W(NO)(CH_2t-Bu)(η^3-DMA) are examined by B3LYP-DFT calculations. Either the mid-H or the methyl H on the DMA can transfer to the W-bound neopentyl to generate neopentane (2,2-dimethylpropane) and Cp*W(NO)(η^2-1,1-dimethylallene) or Cp*W(NO)(η^2-2-methylbuta-1,3-diene) intermediates, respectively. The open coordination site created by the neopentane loss is the site of the subsequent C−H bond activation of alkanes and arenes. The similarities in the overall enthalpic barriers for these mechanisms, 23−24 kcal/mol, explain the observed deuterium distribution (65% on the mid-carbon and 35% on the methyls of the DMA) when benzene-d_6 reacts as substrate.

Introduction

Experimental and theoretical studies of carbon−hydrogen bond activation are one of the most active areas of transition metal chemistry.[1−11] Generally, both stoichiometric and catalytic transition-metal-mediated C−H activation of alkanes or arenes can be classified as one of three types: (1) oxidative-addition by late transition-metal (Ir, Rh, Pt, etc.) complexes; (2) σ-bond metathesis by lanthanide and actinide complexes; and (3) addition of C−H across M−X multiple bonds in early- to mid-transition-metal complexes. On the basis of this variability, complexes have been designed and synthesized in attempts to improve the efficiency of catalysis and to create specific functionality.

Legzdins and co-workers have reported a number of interesting C−H bond activations based on Cp*W(NO)-R′R″ complexes (Scheme 1),[12−16] in which H is transferred from R′ to R″ to create the highly unsaturated intermediates (**b**) that have been trapped by phosphine or pyridine for reactions **I** and **II**. These unsaturated intermediates (**b**) are believed to be responsible for the subsequent C−H bond activations, as alkane or arene molecules can react with intermediates **b** at the empty

Scheme 1

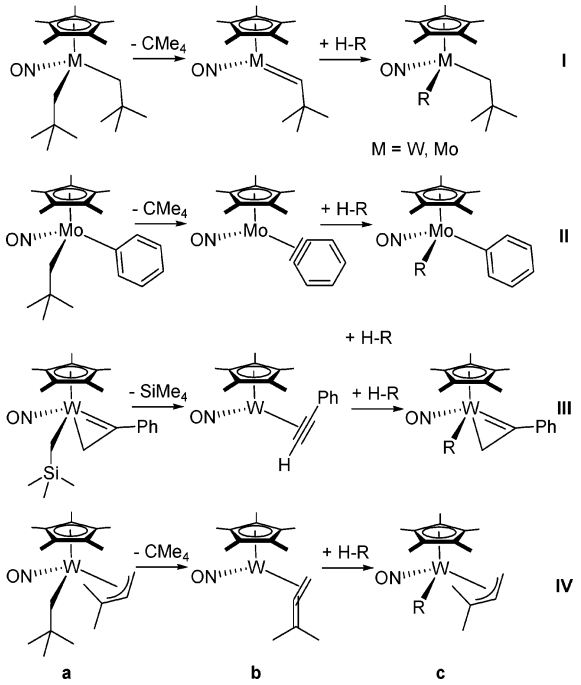

* To whom correspondence should be addressed. E-mail: mbhall@tamu.edu.

(1) *Activation and Functionalization of C−H Bonds*; Goldberg, K. I.; Goldman, A. S.; Eds.; ACS Symp. Ser.; American Chemical Society: Washington DC, 2004; p 885.
(2) Crabtree, R. H. *The Organometallic Chemistry of the Transition Metals*; Wiley-Interscience: New York, 2001.
(3) *Activation of Unreactive Bonds and Organic Synthesis*; Murai, S., Ed.; Springer: Berlin, Germany, 1999.
(4) Labinger, J. A.; Bercaw, J. E. *Nature* **2002**, *417*, 507−514.
(5) Crabtree, R. H. *J. Chem. Soc., Dalton Trans.* **2001**, 2437−2450.
(6) Stahl, S. S.; Labinger, J. A.; Bercaw, J. E. *Angew. Chem., Int. Ed.* **1998**, *37*, 2180−2192.
(7) Shilov, A. E.; Shul'pin, G. B. *Chem. Rev.* **1997**, *97*, 2879−2932.
(8) Crabtree, R. H. *Chem. Rev.* **1995**, *95*, 987−1007.
(9) Arndtsen, B. A.; Bergman, R. G.; Mobley, T. A.; Peterson, T. H. *Acc. Chem. Res.* **1995**, *28*, 154−162.
(10) Crabtree, R. H. *Chem. Rev.* **1985**, *85*, 245−269.
(11) Niu, S.; Hall, M. B. *Chem. Rev.* **2000**, *100*, 353−406.
(12) Pamplin, C. B.; Legzdins, P. *Acc. Chem. Res.* **2003**, *36*, 223−233.
(13) Hayton, T. W.; Legzdins, P.; Sharp, W. B. *Chem. Rev.* **2002**, *102*, 935−991.
(14) Wada, K.; Pamplin, C. B.; Legzdins, P.; Patrick, B. O.; Tsyba, I.; Bau, R. *J. Am. Chem. Soc.* **2003**, *125*, 7035−7048.

10.1021/om049046h CCC: $30.25
Publication on Web 07/06/2005

Scheme 2

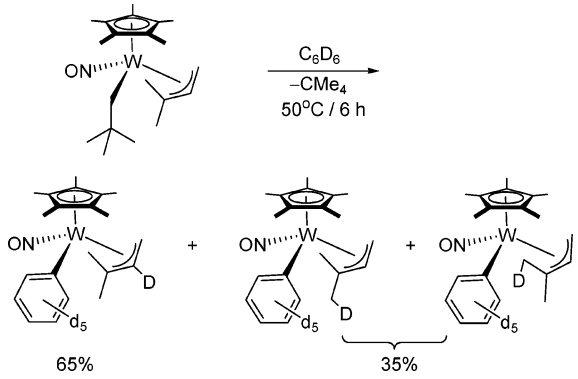

coordination site left by neopentane (or silane) loss and transfer a hydrogen from the substrate (R−H) to the unsaturated ligand in **b**. We have previously examined model systems related to the initial H-transfer in reaction **I** of Scheme 1.[17] Although our prediction that the H-transfer proceeds through a single transition state suggests a σ-bond metathesis mechanism, we noted that the transition state has a particularly short W−H bond. In other work on metal-catalyzed hydroboration we also noted a particularly strong M−H interaction even in cases where the nature of the critical points suggests σ-bond metathesis, and we referred to these reactions as "metal-assisted σ-bond metathesis".[18,19] Maron et al. also noted particularly short M−H contacts even in traditional σ-bond metathesis by La.[20] Recently, Oxgaard et al. described this phenomenon in Ir reactions and suggested the name "oxidative hydrogen migration".[21,22]

Recently, Legzdins and co-workers reported a new reagent, Cp*W(NO)(CH_2t-Bu)(η^3-DMA) (Cp* = η^5-pentamethylcyclopentadienyl and DMA = $H_2CCHCMe_2$), which can initiate the thermal activation of both alkyl and aryl C−H bonds (reaction **IV** in Scheme 1)[23,24] as the latest member of this reaction series. The η^2-allene complex (**IVb**), which can be captured by phosphine, is proposed to form as the active intermediate, which subsequently receives the H from RH to re-form the allyl and the substrate to metal bond (**IV** in Scheme 1). Although formation of the allene intermediate seems to provide a reasonable mechanism, one can infer a more complicated mechanism from isotopic (H vs D) experiments. Reaction with deuterated benzene introduces a deuterium not only on the mid-carbon of the allyl but also on the methyl groups (Scheme 2).[23] From the

Scheme 3

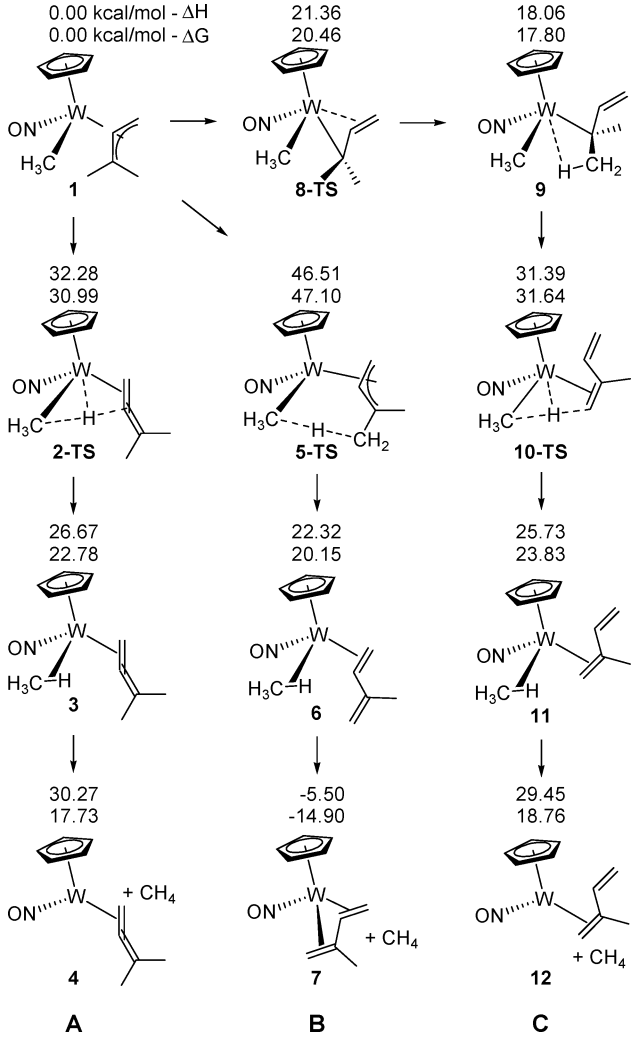

deuterium distribution in the products, Legzdins and co-workers inferred the formation of an intermediate with a 2-methylbut-1,3-diene (MBDE) ligand as well as one with an allene ligand.[23,24] Moreover, NMR experiments suggest that the two methyls on the DMA are exchanged fairly rapidly even at room temperature.[23] Unlike the H-transfer process from the mid-carbon to the neopentyl carbon, there are several puzzles in the H-transfers for the methyl hydrogens in the DMA ligand: (1) does W assist this transfer and if so, how; (2) how can a strongly bound η^3-DMA ligand change into a weakly bound η^2-MBDE ligand and how does the W participate in the transformation; (3) what prevents formation of the very stable η^4-MBDE complex (see structure **7** in Scheme 3), which, when prepared independently, is shown not to react with benzene-d_6 under the same reaction condition?[23]

Computational Details

The theoretical calculations were carried out using the Gaussian 03[25] implementation of B3LYP[26,27] density functional theory (DFT). In the calculations, the Cp* and neopentyl are modeled by cyclopentadienyl (Cp) and methyl, respectively. The basis set for tungsten was modified LANL2DZ (341/341/21) with effective core potentials (ECP),[28,29] where the two outermost p functions were replaced by a (41) split of the optimized tungsten 6p function,[30] and an f function[31] is added.

(15) Adams, C. S.; Legzdins, P.; McNeil, W. S. *Organometallics* **2001**, *20*, 4939−4955.
(16) Poli, R.; Smith, K. M. *Organometallics* **2000**, *19*, 2858−2867.
(17) Fan, Y.; Hall, M. B. *J. Chem. Soc., Dalton Trans.* **2002**, 713−718.
(18) Hartwig, J. F.; Cook, K. S.; Hapke, M.; Incarvito, C. D.; Fan, Y.; Webster, C. E.; Hall, M. B. *J. Am. Chem. Soc.* **2005**, *127*, 2538−2552.
(19) Webster, C. E.; Fan, Y.; Hall, M. B.; Kunz, D.; Hartwig, J. F. *J. Am. Chem. Soc.* **2003**, *125*, 858−859.
(20) Maron, L.; Perrin, L.; Eisenstein, O. *J. Chem. Soc., Dalton Trans.* **2002**, 534−539.
(21) Oxgaard, J.; Muller, R. P.; Goddard, W. A.; Periana, R. A. *J. Am. Chem. Soc.* **2004**, *126*, 352−363.
(22) Oxgaard, J.; Periana, R. A.; Goddard, W. A. *J. Am. Chem. Soc.* **2004**, *126*, 11658−11665.
(23) Ng, S. H. K.; Adams, C. S.; Hayton, T. W.; Legzdins, P.; Patrick, B. O. *J. Am. Chem. Soc.* **2003**, *125*, 15210−15223.
(24) Ng, S. H. K.; Adams, C. S.; Legzdins, P. *J. Am. Chem. Soc.* **2002**, *124*, 9380−9381.

6-31G(d′,p′) basis sets were used for C, N, O, and all H atoms on the methyl and the dimethylallyl, while 6-31G was used for H atoms on the cyclopentadienyl.[32−34] This basis set combination is defined as BS-I. All structures were fully optimized, and frequency analyses were performed to ensure that a minimum or transition state was achieved. The corresponding thermodynamic functions were calculated at the conditions of 298.15 K and 1 atm.

To validate the result based on the truncated model, the real model, including Cp* and neopentyl, was calculated for selected cases with B3LYP. 6-31G(d′) and 6-31G basis sets were used for the carbon and hydrogen atoms on the methyls of the Cp* and the *t*-Bu, respectively, while the same basis sets for the simplified model were employed for the rest.

Furthermore, OLYP/BS-I,[27,35] O3LYP/BS-I,[27,35,36] PBE/BS-I,[37] and TPSS/BS-I[38] were used to do optimization and frequency analyses with thermodynamic function calculations for selected reaction paths. To examine basis set effect, a large basis set combination, in which the SDD/ECP[39] with one f function[31] was used for W while 6-311+(d,p)[32−34] were used for all other main group elements (BS-II), was also implemented with B3LYP and TPSS to calculate the selected cases. Density fitting functions also were tested for BS-I and BS-II with TPSS to check the speedup and calculation quality.[40,41]

Results and Discussion

The B3LYP-DFT calculations show that the methyl can be eliminated as methane by transferring one hydrogen from the DMA ligand by three different routes (**A**, **B**, and **C** in Scheme 3): (1) from the mid-carbon of the DMA mediated by W (**A**); (2) directly from the methyls on the DMA unassisted by W (**B**); or (3) from the methyls in two steps assisted by W (**C**). Routes **A** and **C** have similar overall barriers, whose values are close to expected values; for example reaction I (Scheme 1) has a measured enthalpic barrier of 27 kcal/mol, and as we will show, these two routes can explain the deuterium distribution in Scheme 2. Mechanism **B** is almost 15 kcal/mol higher in enthalpy than either **A** or **C**, so that it is unlikely to be involved at the experimental conditions, although it may be important under other circumstances. The relative enthalpies and the free energies based on the harmonic approximation are also listed in Scheme 3, and the three mechanisms are described in more detail below.

Scheme 4. Mechanism A

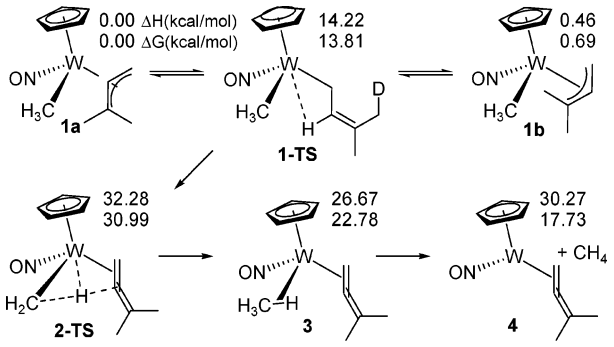

Mechanism A. The allyl complex **1** exists in both *exo*- and *endo*-conformations, **1a** and **1b**, respectively (Scheme 4). **1a** is slightly more stable than **1b** (∼0.5 kcal/mol). The transformation between these isomers occurs through an η^1-allyl, in which the hydrogen on the mid-carbon interacts agostically with W, **1-TS**. The stability of the different conformations and their energy difference depend on the other alkyl or aryl substituent on W; for example, in Cp*W(NO)(R)(η^3-DMA) the dimethylallyl is *endo* for R = CH_2SiMe_3 and it is *exo* for R = $CH_2C_6H_3$-3,5-Me_2 or C_6H_5.[23,24] As shown in Scheme 4, the hydrogen on the mid-carbon of the allyl in **1a** transfers to the methyl through the transition state **2-TS** with an enthalpic barrier of 32.3 kcal/mol. The direct connection between **1-TS** and **2-TS** is confirmed with the intrinsic reaction coordinate (IRC) calculations for **2-TS**.[42,43] The resulting σ-complex **3** easily releases methane by breaking the weak "agostic" bond, a favorable free-energy step to generate the allene complex **4**. The latter complex is 17.7 kcal/mol less stable than **1** at the "standard-state" free energy, but its existence is proven by its capture with PMe_3 to produce the isolated trimethylphosphine complex [Cp*W(NO)(PMe_3)(η^2-H_2C=C=CMe_2)].[23,24]

The 3D structures in Figure 1 and structural parameters listed in Table 1 provide a detailed structural view of the key species in mechanism **A**. Although the DMA in **1a** and **1b** is formally an η^3-ligand, C1 is only weakly bonded to W, as indicated by the W−C1 bond length of 2.7−2.8 Å, which is more than 0.3−0.4 Å longer than those of W−C2 or W−C3. This loose binding eases both the interconversion of **1a** and **1b** and the H-transfer process from C2 because in both **1-TS** and **2-TS** the two methyls on C1 need to rotate away from W. Because of the orthogonal nature of the two coordinates involved in **1-TS** and **2-TS** (rotation of allyl and H transfer), the

(25) Frisch, M. J.; Trucks, G. W.; Schlegel, H. B.; Scuseria, G. E.; Robb, M. A.; Cheeseman, J. R.; Montgomery, J. A., Jr.; Vreven, T.; Kudin, K. N.; Burant, J. C.; Millam, J. M.; Iyengar, S. S.; Tomasi, J.; Barone, V.; Mennucci, B.; Cossi, M.; Scalmani, G.; Rega, N.; Petersson, G. A.; Nakatsuji, H.; Hada, M.; Ehara, M.; Toyota, K.; Fukuda, R.; Hasegawa, J.; Ishida, M.; Nakajima, T.; Honda, Y.; Kitao, O.; Nakai, H.; Klene, M.; Li, X.; Knox, J. E.; Hratchian, H. P.; Cross, J. B.; Adamo, C.; Jaramillo, J.; Gomperts, R.; Stratmann, R. E.; Yazyev, O.; Austin, A. J.; Cammi, R.; Pomelli, C.; Ochterski, J. W.; Ayala, P. Y.; Morokuma, K.; Voth, G. A.; Salvador, P.; Dannenberg, J. J.; Zakrzewski, V. G.; Dapprich, S.; Daniels, A. D.; Strain, M. C.; Farkas, O.; Malick, D. K.; Rabuck, A. D.; Raghavachari, K.; Foresman, J. B.; Ortiz, J. V.; Cui, Q.; Baboul, A. G.; Clifford, S.; Cioslowski, J.; Stefanov, B. B.; Liu, G.; Liashenko, A.; Piskorz, P.; Komaromi, I.; Martin, R. L.; Fox, D. J.; Keith, T.; Al-Laham, M. A.; Peng, C. Y.; Nanayakkara, A.; Challacombe, M.; Gill, P. M. W.; Johnson, B.; Chen, W.; Wong, M. W.; Gonzalez, C.; Pople, J. A. *Gaussian 03*, Revision B.4, B.5, and C.1; Gaussian, Inc.: Pittsburgh, PA, 2003.
(26) Becke, A. D. *J. Chem. Phys.* **1993**, *98*, 5648−5652.
(27) Lee, C.; Yang, W.; Parr, R. G. *Phys. Rev.* **1988**, *37*, 785−789.
(28) Hay, P. J.; Wadt, W. R. *J. Chem. Phys.* **1985**, *82*, 270−283.
(29) Hay, P. J.; Wadt, W. R. *J. Chem. Phys.* **1985**, *82*, 299−310.
(30) Couty, M.; Hall, M. B. *J. Comput. Chem.* **1996**, *17*, 1359−1370.
(31) Ehlers, A. W.; Boehme, M.; Dapprich, S.; Gobbi, A.; Hoellwarth, A.; Jonas, V.; Koehler, K. F.; Stegmann, R.; Veldkamp, A.; Frenking, G. *Chem. Phys. Lett.* **1993**, *208*, 111−114.
(32) Hariharan, P. C.; Pople, J. A. *Theor. Chim. Acta* **1973**, *28*, 213−222.
(33) Petersson, G. A.; Al-Laham, M. A. *J. Chem. Phys.* **1991**, *94*, 6081−6090.
(34) Petersson, G. A.; Bennett, A.; Tensfeldt, T. G.; Al-Laham, M. A.; Shirley, W. A.; Mantzaris, J. *J. Chem. Phys.* **1988**, *89*, 2193−2218.
(35) Handy, N. C.; Cohen, A. J. *Mol. Phys.* **2001**, *99*, 403−412.
(36) Hoe, W.-M.; Cohen, A. J.; Handy, N. C. *Chem. Phys. Lett.* **2001**, *341*, 319−328.
(37) Perdew, J. P.; K. Burke, K.; Ernzerhof, M. *Phys. Rev. Lett.* **1996**, *77*, 3865−3868.
(38) Tao, J.; Perdew, J. P.; Staroverov, V. N.; Scuseria, G. E. *Phys. Rev. Lett.* **2003**, *91*, 146401-1−146401-4.
(39) Dolg, M.; Wedig, U.; Stoll, H.; Preuss, H. *J. Chem. Phys.* **1987**, *86*, 866−872.
(40) Dunlap, B. I. *J. Chem. Phys.* **1983**, *78*, 3140−3142.
(41) Dunlap, B. I. *J. Mol. Struct. Theochem*. **2000**, *529*, 37−40.
(42) Gonzalez, C.; Schlegel, H. B. *J. Phys. Chem.* **1990**, *94*, 5523−5527.
(43) Gonzalez, C.; Schlegel, H. B. *J. Chem. Phys.* **1989**, *90*, 2154−2161.

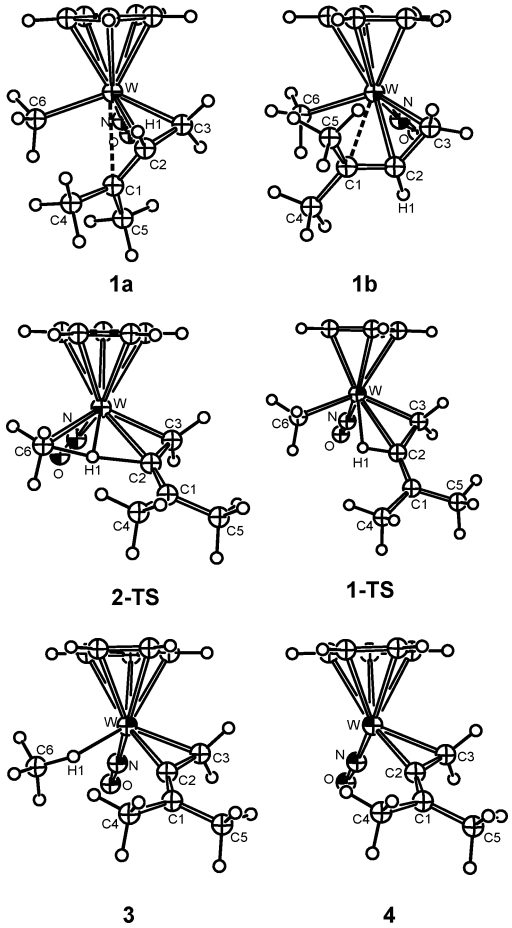

Figure 1. Structures of the species in mechanism **A**.

Table 1. Structural Parameters (bond lengths in Å and bond angles in deg) of the Species in Figure 1

	1a	1b	2-TS	3	4	1-TS
W−C1	2.811	2.721	3.462	3.367	3.311	
W−C2	2.384	2.396	2.205	2.119	2.071	2.489
W−C3	2.230	2.228	2.183	2.180	2.169	2.174
W−C6	2.221	2.219	2.365	2.797		2.218
W−H1	2.887	2.931	1.785	2.046		2.068
C1−C2	1.382	1.384	1.345	1.344	1.344	1.344
C2−C3	1.448	1.447	1.443	1.450	1.470	1.481
C2−H1	1.092	1.090	1.637	2.541		1.132
C6−H1	3.735	3.707	1.400	1.128		2.239
C1−C2−C3	125.9	123.8	135.0	134.8	135.2	133.3

reaction coordinate from **2-TS** back to the reactants (**1**) bifurcates through **1-TS**. The migrating H in **2-TS** is 1.785 Å away from W, which is almost the same as the W−H bond length in the transition state calculated for the H-migration reaction between the methyl groups in $Cp^*W(NO)(CH_3)_2$ or $CpW(NO)(CH_3)_2$ in a model for reaction **I** in Scheme 1,[17] and this H, the W, and the two adjacent C atoms are nearly planar (C2−W−H1−C6 = 176.3°). In the σ-complex **3**, the interaction between methane and W is a typical agostic bond involving both H1 and C6, and the C6−H1 bond is lengthened by 0.03 Å compared to the normal C−H bond in methane. The rest of the geometry in **3** is very similar to that in **2-TS**, consistent with **2-TS** being a very late transition state as expected from Hammond's postulate. Apart from methane loss, the structure of **4** is also very similar to **3**. However, because **4** is coordinately unsaturated, the bonding between W and the allene is stronger in **4**, in which both W−C2 and W−C3 are shorter and C2−C3 is longer than those in **3** (Table 1).

Scheme 5. Mechanism B

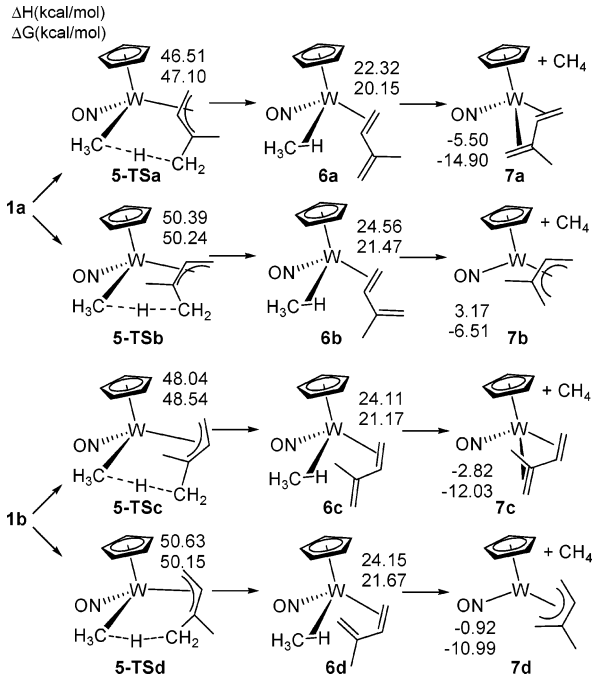

Mechanism B. Although this route appears to be higher in energy than either **A** or **C**, we will describe it in some detail because of its close relation to the two low-energy routes, especially **C**. Furthermore, the product of this route, synthesized in different reactions, has been isolated and structurally characterized. In this mechanism a hydrogen atom from one of the methyl groups of the DMA transfers directly to the methyl bound to W. As shown in Scheme 5 and Figure 2, there are four paths in this mechanism since the allyl ligand has *exo*- and *endo*-conformations and the DMA has two methyl groups that can be differentiated in the H-transfer process.[44] Some key structural parameters of the species in Figure 2 are also listed in Table 2.

In all four of the transition states (**5-TS**) for the H-transfer, the metathesizing H is about 2.8 Å away from W, long enough so that there is no interaction between this H and W in this transfer process. As expected for this type of transfer, the barrier is high, >48 kcal/mol in enthalpy, a value that is 15 kcal/mol higher than that in mechanism **A**. In the resulting σ-complexes (**6**) the DMA ligand is transformed into *trans*- or *cis*-2-methylbut-1,3-diene (MBDE). Moreover, the methane's agostic H in **6** is not the H transferred from the DMA because another H (H3 in Figure 2) on the W-bound methyl (methane) forms an agostic bond in **5-TS** (and **6**). Again in **6** the methane is weakly bound to W, and it can be easily released. Finally, the uncoordinated C−C double bond in the MBDE is oriented toward the open site created by the methane loss and can form a second "π" dative bond to W in the products, **7**. These η^4-diene complexes (**7**) are up to 15 kcal/mol more stable than **1** in free energy. Interest-

(44) Due to the steorochemical difference of the two methyls on the DMA, the methyls are differentiated as *cis* and *trans* and the methyl closer to the Cp is defined as *cis*-Me and the methyl farther as *trans*-Me.

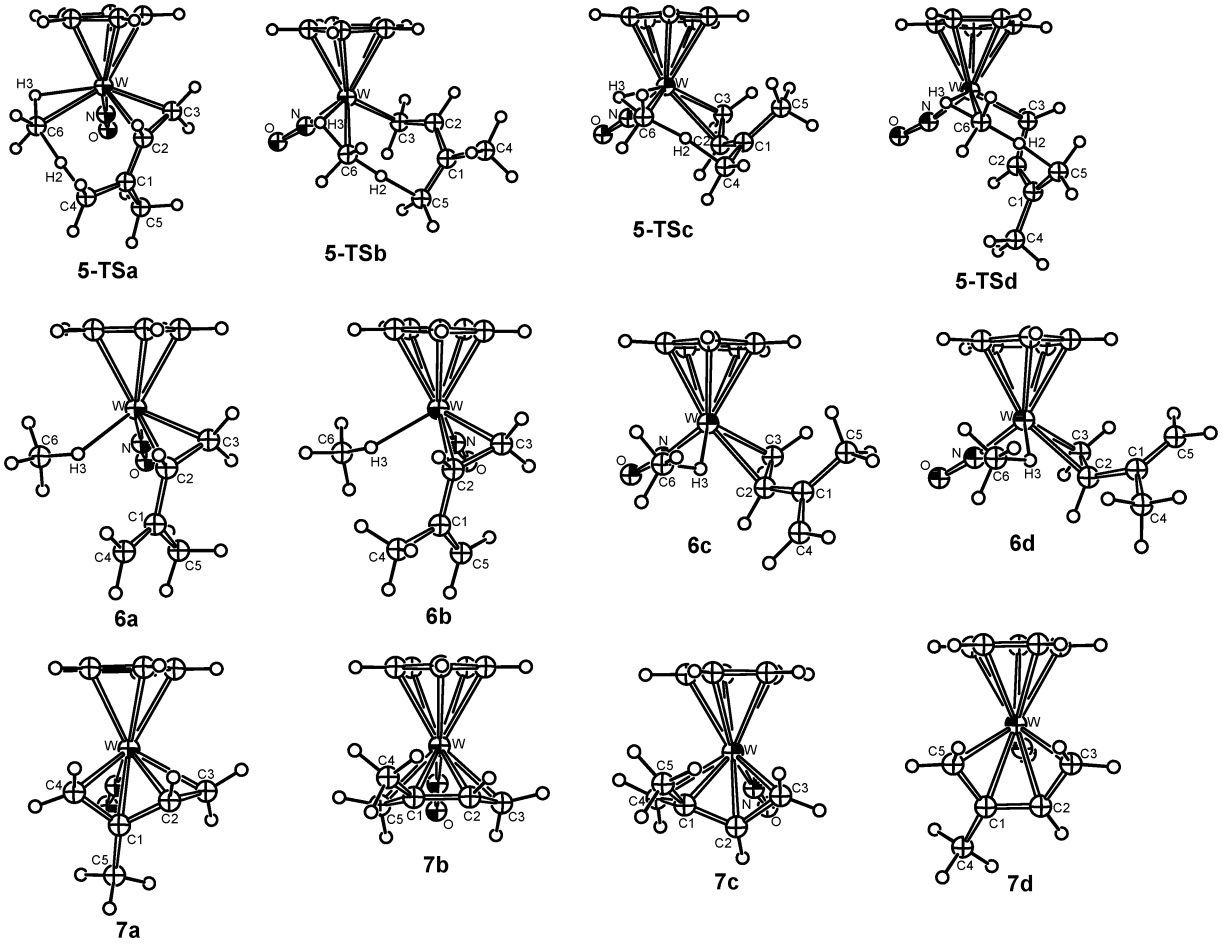

Figure 2. Structures of the species in mechanism **B**.

Table 2. Structural Parameters (bond lengths in Å and bond angles in deg) of the Species in Figure 2

	5-TSa	5-TSb	5-TSc	5-TSd	6a	6b	6c	6d
W−C1	3.087	3.504	3.107	3.513	3.261	3.263	3.295	3.256
W−C2	2.356	2.742	2.396	2.732	2.246	2.241	2.259	2.242
W−C3	2.212	2.252	2.210	2.239	2.189	2.180	2.183	2.176
W−C4	3.743	4.573	3.772	4.594	4.218	4.335	4.248	4.187
W−C5	3.763	3.766	3.782	3.752	3.855	3.810	3.914	3.948
W−C6	2.383	2.303	2.375	2.299	2.748	2.761	2.736	2.751
W−H2	2.818	2.745	2.850	2.780				
W−H3	2.038	1.829	1.984	1.834	2.011	2.030	2.044	2.041
C1−C2	1.418	1.403	1.413	1.402	1.489	1.494	1.488	1.494
C2−C3	1.450	1.442	1.450	1.441	1.455	1.458	1.456	1.458
C1−C4	1.408	1.516	1.411	1.515	1.347	1.515	1.347	1.514
C1−C5	1.511	1.404	1.512	1.407	1.511	1.344	1.512	1.346
C4−H2	1.402		1.406					
C5−H2		1.479		1.457				
C6−H2	1.380	1.275	1.380	1.294				
C6−H3					1.129	1.130	1.128	1.129
C1−C2−C3	126.5	128.7	127.5	128.3	124.6	124.4	124.6	123.1

ingly, the η^4-*trans*-MBDE complexes are more stable than the *cis*- mainly because the *trans*-MBDE is more flexible so that it better occupies the pseudo-octahedral coordinate sites available on W.

Since the barriers for H transfer in mechanism **B** are all much higher than those of mechanism **A**, mechanism **B** cannot explain the 35% deuterated methyl products observed in the isotope experiment. Moreover, this reaction produces only very stable η^4-diene complexes **7**, which in other experiments have been shown not to react with benzene-d_6.[23] Thus, the observed deuterated methyl products must be produced through another mechanism.

Mechanism C. As shown in Scheme 6, Figure 3, and Table 3 the η^3-DMA in **1a** or **1b** can change to η^1, in which the vinyl end is uncoordinated, via **8-TS** with an enthalpic barrier of 20−21 kcal/mol. According to the structures of **8-TSa** and **8-TSb** (Figure 3 and Table 3), C2 is far from W (2.8−2.9 Å). Then, one of the hydrogen atoms on one of the methyls of the DMA can interact with W to form **9** with a β-H agostic bond (Figure 4 and Table 3). In **9**, the agostic W−H and W−C distances are 2.02−2.09 and 2.50−2.53 Å, respectively, and the C−H bond length increases by ∼0.04 Å compared to the original C−H bond in **1**. This agostic H in **9** then transfers to the W-bound methyl to form the σ-complex **11**. In the transition states (**10-TS**) connecting **9** and **11**, the transferring H is ∼1.785 Å away from W; thus, W assists the transfer and reduces the enthalpic barrier to 31−35 kcal/mol. Although **11** and **6** appear to have similar structures, the unbound vinyl is oriented away from the methane site so that this vinyl will not easily close the open site left by methane loss. The barrier for the rotation from **12** to **7** is about 10 kcal/mol in enthalpy (rotational TSs in Scheme 6), so the reactive intermediates **12** prefer capturing an alkane or arene molecule to rotating. Thus, the overall enthalpic barrier for this mechanism (**C**) is to 31.4 kcal/mol, very close to that of mechanism **A**, while mechanism **B** is at least 15 kcal/mol higher energy (Scheme 3 and Figure 5).

Of the three mechanisms, mechanisms **A** and **C** have similar overall barriers in enthalpy (Figure 5) and free energy, and the reactive intermediates derived from

Scheme 6. Mechanism C[a]

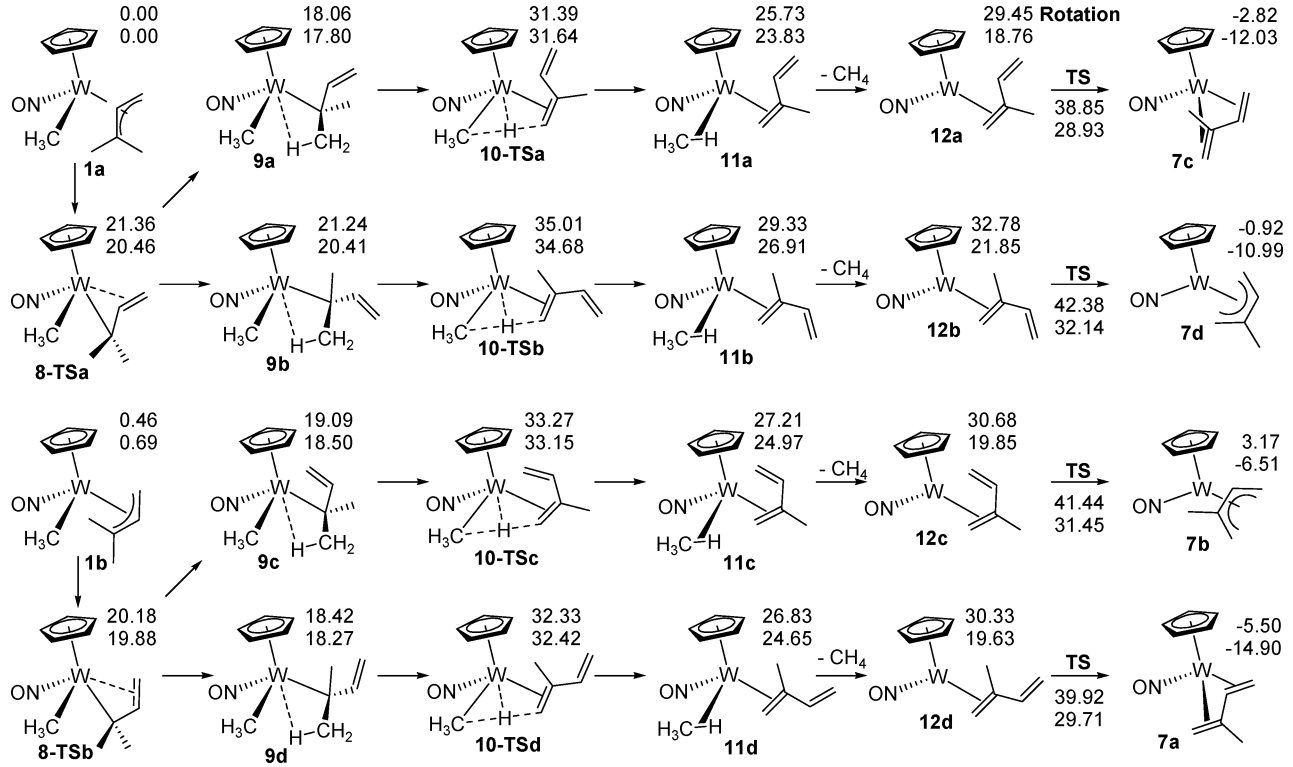

[a] Methane was added to **12**, **TS** (rotation), and **7** when the relative enthalpies and free energies were computed.

Table 3. Structural Parameters (bond lengths in Å and bond angles in deg) of the Species in Figures 3 and 4

	8-TSa	8-TSb	9a	9b	9c	9d	10-TSa	10-TSb	10-TSc	10-TSd
W−C1	2.205	2.196	2.223	2.211	2.214	2.210	2.247	2.235	2.242	2.242
W−C2	2.900	2.784	3.168	3.153	3.147	3.121	3.178	3.156	3.203	3.124
W−C3	3.648	3.630	4.290	3.996	3.859	4.225	4.304	4.005	4.000	4.248
W−C4	3.122	3.143	2.499	3.238	3.225	2.504	2.279	3.263	3.219	2.278
W−C5	3.137	3.156	3.214	2.510	2.525	3.220	3.217	2.284	2.282	3.261
W−C6	2.140	2.151	2.222	2.220	2.215	2.217	2.368	2.369	2.371	2.364
W−H2			2.024	2.049	2.094	2.059	1.785	1.786	1.784	1.785
C1−C2	1.507	1.501	1.493	1.495	1.495	1.488	1.486	1.493	1.492	1.485
C2−C3	1.344	1.348	1.342	1.338	1.342	1.342	1.342	1.338	1.341	1.342
C1−C4	1.547	1.545	1.527	1.540	1.535	1.526	1.473	1.533	1.532	1.472
C1−C5	1.542	1.540	1.530	1.521	1.524	1.534	1.525	1.466	1.466	1.528
C4−H2			1.140			1.140	1.595			1.596
C5−H2				1.140	1.134			1.592	1.589	
C6−H2			2.198	2.187	2.218	2.205	1.402	1.400	1.401	1.401
C1−C2−C3	128.1	128.0	127.6	129.7	129.2	127.0	127.3	128.4	129.3	126.8

methane loss, **4** and **12**, have similar stability. These intermediates can then react with deuterated alkanes or arenes following the mechanistic steps in reverse.

Exchange of Two Methyl Groups on DMA. As shown in Scheme 7, the labeled H (D) can be differentiated in four conformational isomers, **1a**, **1a′**, **1b**, and **1b′** (Scheme 7). **1a** and **1b** (or **1a′** and **1b′**) can transform to the other conformer via transition state **1-TS**, in which the hydrogen on the mid-carbon interacts agostically with W to stabilize this transition state (Figure 1 and Table 1). The activation enthalpy for **1-TS** is only 14.2 kcal/mol, while the exchange between **1a** and **1b′** (or **1a′** and **1b**) is a stepwise process, proceeding through η^3- to η^1-allyl, rotation of vinyl, and η^1- to η^3-allyl with an overall enthalpic barrier of 24.7 kcal/mol.

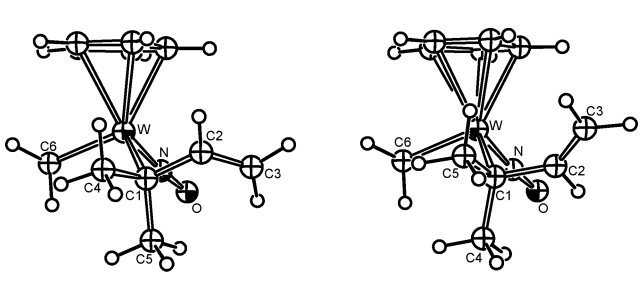

Figure 3. Structures of the species in mechanism **C**.

Although 24.7 kcal/mol is slightly too high for a fast process at room temperature, this barrier is ∼7 kcal/mol lower than the barrier for the C−H activations in mechanisms **A** and **C**, which occur at 50 °C. Thus, the H/D exchange process shown above is most likely viable at room temperature.

Density Functional Methods and Basis Set Effects on Mechanism A. To examine how sensitive our predictions are to the methodology, several newer functionals, OLYP, O3LYP, PBE, and TPSS, and larger basis sets (BS-II) were employed to reoptimize all

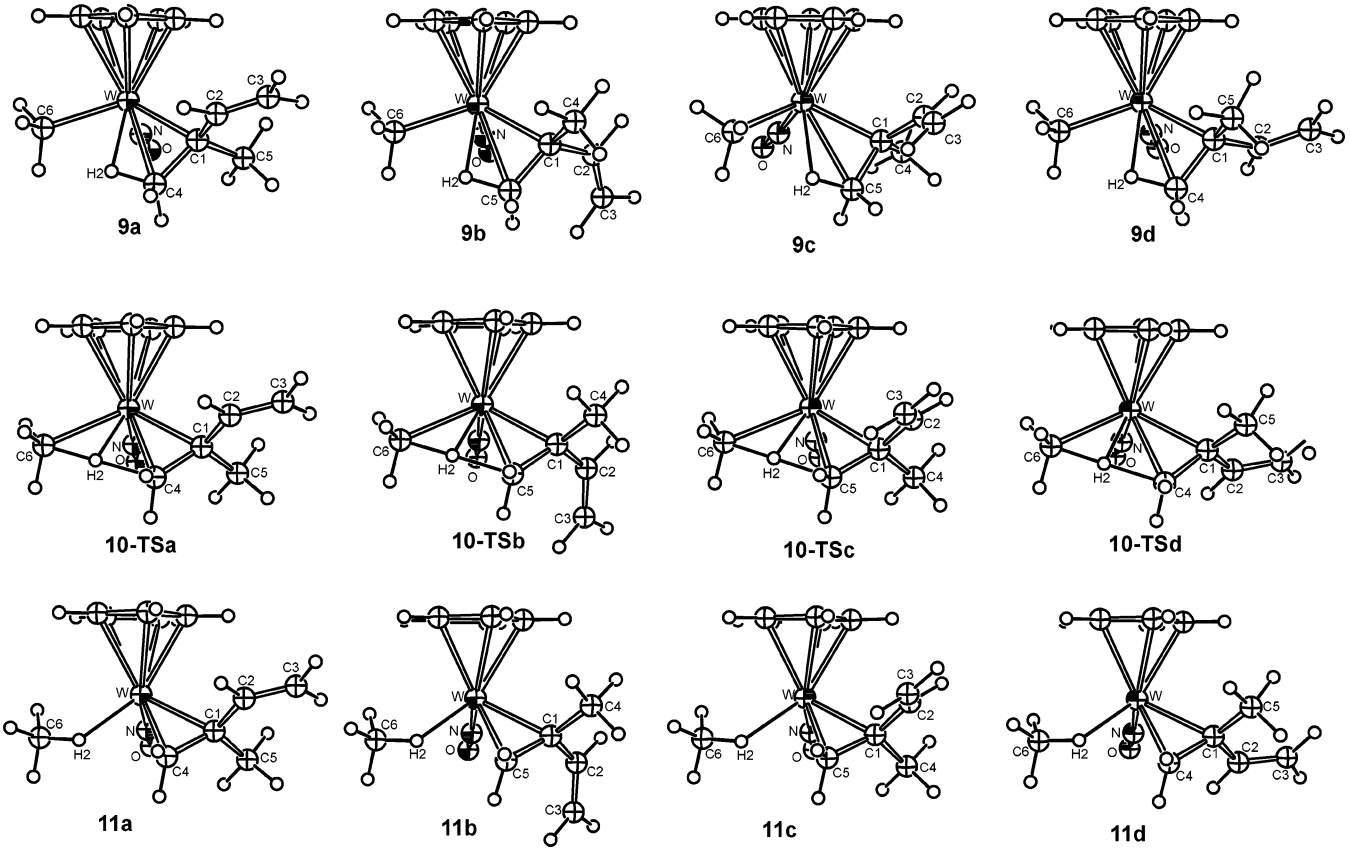

Figure 4. Structures of the species in mechanism **C**.

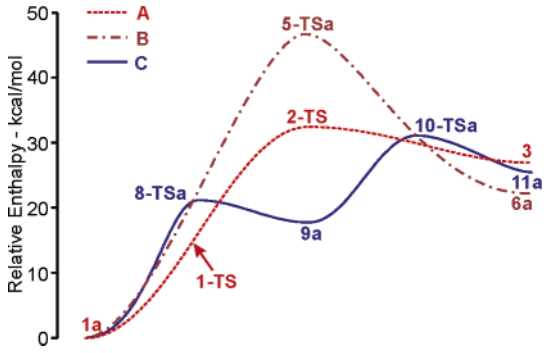

Figure 5. Reaction profiles for mechanisms **A**–**C**.

species in mechanism **A** (Scheme 4 and Figure 1). Although the similarity of the results for different functionals is not proof that the predictions are correct, it provides some confidence that there are no hidden pathological problems.

Of the relative energies listed in Table 4, OLYP, O3LYP, and PBE slightly prefer **1a** to **1b** by 0.3–0.6 kcal/mol in free energy, very close to B3LYP's result, while TPSS indicates they have almost the same stabilities. For the H-transfer barrier (**2-TS**), all other DFT methods predict a lower energy barrier for the H-transfer (**2-TS**) than B3LYP's by at least 3 kcal/mol in free energy, especially for OLYP, which has an 8 kcal/mol lower barrier. Although pure DFT functionals usually underestimate reaction barriers, O3LYP (hybrid DFT) and TPSS (pure DFT with meta-GGA) are expected to be very close in quality to B3LYP,[38,47,48] which suggests that the B3LYP's barrier may be slightly too high. In **3**, the agostic bonding enthalpy varies significantly based on different DFT methods: B3LYP gives a rather weak agostic interaction, 2.8 kcal/mol; OLYP and O3LYP predict a 1–3 kcal/mol repulsion between CH_4 and the CpW(NO)(DMA) moiety though their structures are very similar to the B3LYP's; PBE and TPSS show much stronger binding enthalpies, 8.27 and

Scheme 7

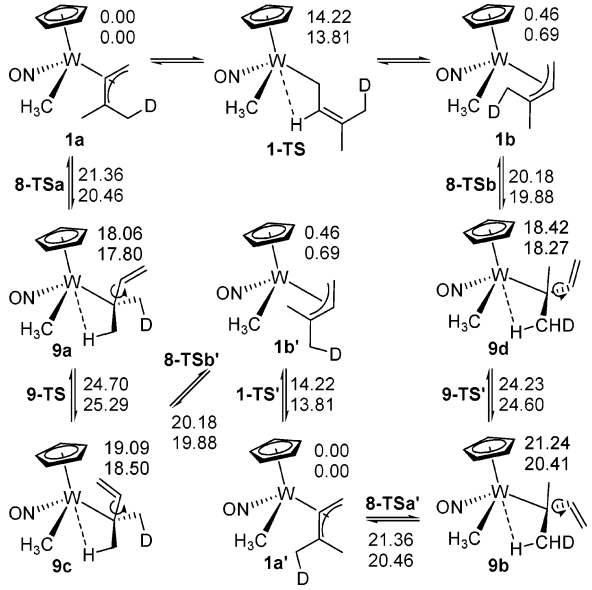

(45) Boys, S. F.; Bernardi, F. *Mol. Phys.* **1970**, *19*, 553–566.
(46) Simon, S.; Duran, M.; Dannenberg, J. J. *J. Chem. Phys.* **1996**, *105*, 11024–11031.
(47) Baker, J.; Pulay, P. *J. Chem. Phys.* **2002**, *117*, 1441–1449.
(48) Baker, J.; Pulay, P. *J. Comput. Chem.* **2003**, *24*, 1184–1191.

Table 4. Density-Functional-Methodological Comparison (BS-I unless otherwise noted) of Relative Enthalpies and Free Energies (kcal/mol) for Mechanism A (Scheme 4 and Figure 1)

	1a		**1b**		**2-TS**		**3**			**4** + CH_4	
functional	ΔH	ΔG	ΔH	ΔG	ΔH	ΔG	ΔH	ΔG	BSSE[a]	ΔH	ΔG
B3LYP	0.00	0.00	0.39	0.66	34.26	32.91	26.82	22.79	1.83	29.66	17.12
B3LYP[b]	0.00	0.00	0.43	0.71	31.45	30.26	24.93	21.80	0.48	27.51	15.32
OLYP	0.00	0.00	0.20	0.57	25.72	24.85	22.57	19.51	1.91	19.95	7.82
O3LYP	0.00	0.00	0.17	0.43	27.90	26.82	24.23	21.15	2.13	23.22	10.89
PBE	0.00	0.00	0.28	0.27	28.50	26.99	27.28	24.37	2.09	35.55	22.49
TPSS	0.00	0.00	0.15	−0.01	31.59	29.91	27.60	24.35	1.66	34.18	21.28
TPSS[c]	0.00	0.00	0.21	0.09	31.71	30.11	27.56	24.45	1.55	34.15	21.43
TPSS[b]	0.00	0.00	−0.02	−0.23	30.75	28.79	26.12	23.09	0.63	32.02	19.02
TPSS[d]	0.00	0.00	−0.03	−0.27	30.71	28.77	26.07	23.04	0.63	32.00	19.01

[a] Basis set superposition error (BSSE) calculated with counterpoise method.[45,46] [b] BS-II. [c] BS-I with density fitting functions. [d] BS-II with density fitting functions.

Table 5. Key Structural Parameters (bond lengths in Å and bond angles and dihedral angles in deg) of 2-TS and 3

	2-TS						**3**			
	W−H1	W−C2	W−C6	C2−H1	C6−H1	C2−W−H1−C6	W−H1	W−C6	C6−H1	W−H1−C6
B3LYP	1.785	2.205	2.365	1.637	1.400	176.3	2.046	2.797	1.128	120.9
B3LYP[a]	1.791	2.223	2.369	1.636	1.412	176.9	2.056	2.772	1.126	118.2
OLYP	1.783	2.186	2.363	1.655	1.380	175.8	2.054	2.786	1.133	119.1
O3LYP	1.778	2.184	2.354	1.643	1.379	176.3	2.043	2.758	1.130	117.8
PBE	1.796	2.182	2.364	1.665	1.374	174.3	1.978	2.628	1.155	111.3
TPSS	1.789	2.191	2.367	1.653	1.407	175.1	1.993	2.675	1.144	114.3
TPSS[b]	1.789	2.192	2.367	1.654	1.408	175.0	1.994	2.675	1.144	114.2
TPSS[a]	1.796	2.208	2.370	1.650	1.419	175.4	2.013	2.678	1.141	113.3
TPSS[c]	1.796	2.209	2.370	1.650	1.420	175.4	2.013	2.679	1.142	113.4

[a] BS-II. [b] BS-I with density fitting functions. [c] BS-II with density functions.

6.58 kcal/mol, respectively. According to both experiments[49] and calculations,[50] the binding enthalpy between CH_4 and $W(CO)_5$ is 4−5 kcal/mol. Assuming the two neutral 16e systems, $W(CO)_5$ and CpW(NO)(DMA), are similar, B3LYP's binding energy is too low while PBE's and TPSS's are too high without BSSE (basis set superposition error) correction, which is about 2 kcal/mol at these theory levels. Furthermore, compared to the calculation of B3LYP/BS-I and TPSS/BS-I, the reaction barrier becomes slightly lower (∼3 and 1 kcal/mol, respectively) when larger basis sets, BS-II, are employed and the agostic interaction is about 0.5−1 kcal/mol weaker. Of course, the reduced agostic binding energy arises primarily because the larger basis produces a smaller BSSE, which is about 0.5 kcal/mol for BS-II.

For most structural parameters, the different DFT calculations produce results very similar to those in Table 5, where we list only structural parameters related to the transferring H in **2-TS** and the agostic bond in **3** (Figure 1). There are no significant differences between the structures optimized with different DFT methods, although stronger agostic interactions are indicated for PBE and TPSS by shorter W−H1 and longer C6−H1 distances.

When density fitting functions are used for either BS-I or BS-II, the TPSS calculations show only marginal differences for both energetics in Table 4 and structural parameters in Table 5, but for this pure DFT method, more than 50% and 70% of the computational time is saved for optimization and frequency calculations, respectively.

In brief, OLYP, O3LYP, and PBE give much lower reaction barriers than B3LYP does, while TPSS predicts only slightly lower. Furthermore, B3LYP is more sensitive to basis sets than TPSS is since the reaction barrier decreases by ∼3 kcal/mol and only ∼1 kcal/mol for B3LYP and TPSS, respectively, when BS-II is employed instead of BS-I. OLYP and O3LYP are unable to calculate the agostic interaction which B3LYP underestimates and PBE overestimates significantly. TPSS also slightly overestimates the agostic interaction, but larger basis sets correct most of this error, while no significant improvement is observed for B3LYP.

Real Model for Mechanisms A and C. Although the calculations based on the truncated model match the experiment quite well, the stronger electron donor strength of Cp* and the steric effects of the methyls on the Cp* and the *t*-Bu in the real system cannot be ignored. Mechanism **A** and the lowest energy branch of mechanism **C** were calculated for the real model. All corresponding intermediates and transition states were fully optimized and confirmed by frequency analysis for the actual system. The corresponding species for these two mechanisms are shown in Scheme 8, and the relative enthalpies and free energies are also listed in kcal/mol.

The full model does not change the mechanisms, although the overall activation enthalpies for these two paths decrease by 3−5 kcal/mol (Scheme 8). Apparently, the better electron donor, Cp*, increases the electron density on W and further stabilizes the transferring hydrogen, which is hydride-like, in the transition states, **2-TS″** and **10-TS″**. The structures of all species shown in Scheme 8 are similar to the simple model, although Cp* rotates to other conformations because of the stronger repulsions between the methyls on the Cp* and

(49) Brown, C. E.; Ishikawa, Y.; Hackett, P. A.; Rayner, D. M. *J. Am. Chem. Soc.* **1990**, *112*, 2530−2536.
(50) Zaric, S.; Hall, M. B. *J. Phys. Chem. A* **1997**, *101*, 4646−4652.

Scheme 8. Relative Enthalpies and Free Energies (in kcal/mol) for Mechanisms A and C[a]

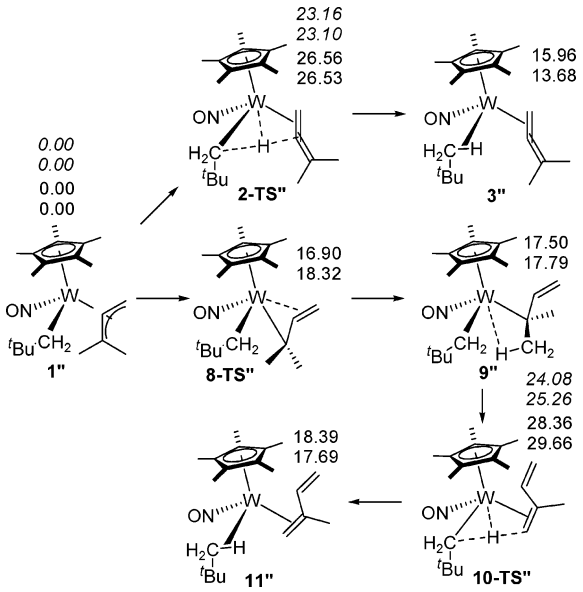

[a] The values in italics are for TPSS/BS-II with density fitting functions.

other ligands. So, the results derived from the simple model are reliable and even quantitatively close to those in the real experiment system.

Furthermore, the basis set effect (BS-II vs BS-I) could lower the reaction barriers by ~3 kcal/mol for B3LYP according to results shown in Table 4. Unfortunately, calculations (especially the frequency analyses) in the very large basis sets such as BS-II are intolerably slow with the B3LYP functional for the real model. With the help of density fitting functions, it is possible to compute the real model with pure DFT in the very large basis sets, BS-II. Here, we repeated the optimization and frequency analyses for **1″**, **2-TS″**, and **10-TS″** at the level of TPSS/BS-II. The enthalpic barriers of 23.2 and 24.1 kcal/mol for mechanisms **A** and **C**, respectively, are consistent with the reaction conditions, 50 °C for 6 h.[12,51] The slightly higher activation enthalpy of mechanism **C**, relative to **A**, matches the isotopic experiment very well.

Conclusion

In conclusion, both the H on the mid-carbon and the hydrogen atoms on the methyls of the dimethylallyl in the tungsten nitrosyl complex can be transferred to the alkyl group to form a σ-alkane ligand as a good leaving group. A reactive intermediate with an allene ligand is produced if the hydrogen on the mid-carbon transfers, while one with an η^2-2-methylbuta-1,3-diene is formed if one of the methyl hydrogens is transferred. Tungsten assists the H-transfer through a "metal-assisted" σ-bond metathesis mechanism, which stabilizes the corresponding transition states significantly. The overall barriers and the stabilities of the reactive intermediates are very close for these two mechanisms (mechanisms **A** and **C**), which together with the low-energy rearrangements in Scheme 7 explains the deuterium distribution of the products in the isotope experiment.[23]

Acknowledgment. We would like to thank the National Science Foundation (Grant No. CHE 98-00184 and MRI 02-16275) and the Welch Foundation (Grant No. A-648) for their generous support. We also appreciate Peter Legzdins for his generous and helpful discussion about his experiments.

OM049046H

(51) In Legzdins and co-workers' kinetic experiments,[12] the activation enthalpies of reaction I (in Scheme 1) for W and Mo complexes are 27.2 ± 1.7 (71−98 °C) and 23.7 ± 0.2 (26−40 °C) kcal/mol, respectively. Compared to the reaction conditions, 70 °C for 40 h, for Cp*W(NO) (CH_2t-Bu)$_2$, the enthalpic barriers of 23−24 kcal/mol are reasonable and consistent with the experimental phenomena.